



## THE INFLUENCE OF THE INTERNAL PRESSURE AND IN-PLANE BENDING MOMENT LOADINGS ON PIPE BENDS

<sup>1</sup>Haidy Salah El-Deen, <sup>2</sup>Ihab Mohamed El-Aghoury, <sup>3</sup>Sherif Kamal Hassan, <sup>4</sup>Diana Abdulhameed

<sup>1</sup>Post graduate student, <sup>2</sup> Associate Professor of structural engineering, <sup>3</sup> Professor of structural engineering, Department of Structural Engineering, Ain Shams University, Cairo, Egypt, <sup>4</sup> Research Engineer Pipeline Integrity & Operations C-FER Technologies, Edmonton, AB Canada,

**Abstract:** Circular thin-walled pipe bends are frequently used as a key part in pipeline connection either in the vertical direction or the horizontal direction due to their high flexibility. The high flexibility of pipe bends is due to the ability of their cross-section to ovalize when subjected to internal pressure and/ or bending moments that lead to high-stress concentrations at bend locations within the pipeline system.

Moreover, the surface geometric characteristics of bends may cause some unbalanced outward forces caused by the induced internal pressure loading only which leads to an outward resultant force that tends to straighten out the bend causing a rise within the deformations and stress levels. This phenomenon was known as "The Bourdon effect". In addition to that, external bending moment load acting on the pipe bends may result from either occasional loadings such as; seismic loads, soil settlement, and/ or secondary loadings exerted on the pipe due to thermal expansions resulted in additional stresses.

These additional stresses resulting from bending loads acting on the pipe bend are accounted for in the design codes using stress intensification factors (i) and flexibility factors (K). These factors are presented in the current American code ASME B31.3. Although they have been derived for a 90-degree pipe bend subjected to in-plane closing bending moment with long bend radius (R), they cannot be used for other loading cases such as in-plane opening moment or out-of-plane bending moment.

Previous studies showed that the direction of bending moment affected the distribution and magnitude of stress levels found on the bend. However, previous studies considered only small pipe sizes of NPS 16 (406mm) and smaller under bend angles of 90 degrees or less. This paper extended the investigation on smooth pipe bends with initial circular cross-sections and uniform wall thickness with large pipe size from NPS20 (508mm) up to NPS 72 (1829mm) under a wide range of bend angles ( $\theta$ ) (from 30° up to 160°).

The loading considered in this study is the internal pressure and the in-plane opening/closing bending moment. In this respect, an extensive parametric study is conducted using a numerical finite element analysis (FEA) simulation using ABAQUS software to model Pipe bends with different nominal pipe sizes (NPS), bend angles ( $\theta$ ), bend wall thickness (t), and various bend radius (R). The results showed that as the bend angle increases, the flexibility of the bend increases as well leading to higher stresses on the pipe bend. Finally, from the finite element analysis results depicted through curves, it could be concluded that the codes do not cover the stress distribution for large pipe bends accurately.

**Key Words -Pipe bends; Bend angle; internal pressure; Finite element analysis (FEA).**

### I. INTRODUCTION

As an imperative detail of the pipeline, pipe bends are significantly used in several enterprise industries (water, oil, and gas) and everyday life commercial productions. The purpose of pipeline systems is to transfer the medium whether it is water, gas, or oil to the processing facility through pipe networks. In the water industry, (either drinking water or wastewater) large-diameter pipes (greater than or equal NPS 20) are increasingly used to discharge natural bodies of water and transmit sewage to a wastewater treatment facility.

These pipe networks consist of many-branched pipelines which are in small diameters known as household branches with diameters from NPS 8 to NPS16 that mainly carry the accumulated flows to their final destination. While, in oil and gas production, and refining industries, the fluids are transmitted through large diameter pipes and distribution pipes which are in small diameters (closer to houses).

Therefore, the objective of this paper is to simulate a certain case of study of pipe bends that existed in a horizontal water pipeline network of 1906 Km made of carbon steel above ground. After the operation of the pipeline, a sudden ground settlement of one of the pipeline supports resulted in crack initiation then crack propagation that leads to the rupture of one of the connecting vital pipe bends and leakage. This ground settlement resulted in the displacement of one of the supports subjecting the pressurized pipe bend to in-plane bending moments in different directions that were expected to lead to that collapse.

Focusing on the effect of that ground settlement on the behavior of large pipe bends, an extensive parametric study is conducted taking into consideration the wide selection of pipe sizes (NPS) from NPS20 (508mm) up to NPS72 (1829mm), with different bend angles ( $\emptyset$ ) ( from 30° up to 160°), and bend radii (R)(R= 1D, 5D), to quantify the effect of bend angle ( $\emptyset$ ) of an initially circular cross-sectional seamless smooth pipe bend of uniform thickness (t) with different pipe bend radius to thickness ratio (r/t) (from 10 to 100) on the stress distribution along with the pipe bend thickness layers( outer, mid and inner layers).

The loading on the pipe bends are found to be, first: the pressure during the induction of the transferred medium to the processing facility branched pipes, and second: the in-plane bending moments( closing and opening) will be studied separately. The effect of the two types of loading is going to be studied separately in this paper to test simultaneously the effect of internal pressure and in-plane bending moment and observe the changes in stiffness, flexibility, stress levels, and test the link between such changes and the cross-section deformation.

In the late 1953's Nicol Gross [1] studied 90-degree short radius bends subjected to internal pressure and closing in-plane bending moment with small pipe bend factor ( $h < 0.3$ ), He showed that the theoretical method based on Von Kármán (1911) [2] assumptions and analysis are invalid for predicting stresses because the latter assumed that the longitudinal stresses are the dominant reason behind the cross-sectional deformation and ignored the circumferential membrane stresses (hoop stresses) for simplicity.

Von Kármán (1911) has introduced in his theoretical stress analysis that pipe bends tend to have higher flexibility than straight pipes and developed a factor that accounts for the increase in flexibility and stresses of pipe bends under closing bending moment known as the "flexibility" and "Stress intensification" factors which are simply the ratios of the actual flexibility and stress of a pipe bend to those predicted of straight pipe by (Barlow's equation ( $\sigma = PD/2t$ )).

Rodabaugh & George (1957) [3] followed Karman's assumptions and derived flexibility factors (K) and stress intensification factors (i), based on bending moment loading only and they're still used without any modifications without taking the effect of bend angle ( $\emptyset$ ), and in-plane bending moment direction(closing and opening) into consideration, however, the internal pressure was considered in the stress intensification factors along with the in-plane bending moment.

## NOMENCLATURE

$\emptyset$ Bend Angle, degrees.	$\nu$ poisson's ratio
$t$ Thickness of pipe	$\sigma_y$ Yield stress
$R$ bend radius, mm	$\sigma_h$ Hoop stress
$L$ length of the attached straight pipe	$\sigma_L$ Longitudinal stress
$R/r$ relative bend radius	FEA Finite Element Analysis
$r/t$ relative thickness	NPS Nominal Pipe Size
$D$ outer diameter of the pipe, mm	$i$ Stress Intensification Factor (SIF)
$P$ applied internal pressure	$M$ In-plane bending moment
$h$ Bend ratio( beam parameter) = $Rt/r^2$	SMS Specified minimum yield strength
$E$ Young's modulus	

## II. METHODOLOGY

### 2.1 The Finite Element modeling technique

The Finite Element Method was used to investigate the current problem using the commercial software package ABAQUS 16.6 [4]. The Finite Element Analysis (FEA) model of the pipe bends considered a range of thin-walled pipes with diameter to wall thickness ratio greater than 20, ( $D/t \geq 20$ ), bend angles ( $\emptyset$ ) varying from 30° to 160°, and bend radius (R) from (1D) to (5D). Two straight pipes of length 10 times the pipe outer diameter ( $L = 10D$ ) are attached to the bend ends to avoid the effect of the end constraints on the pipe bend stress distribution, as shown in Fig. (1)

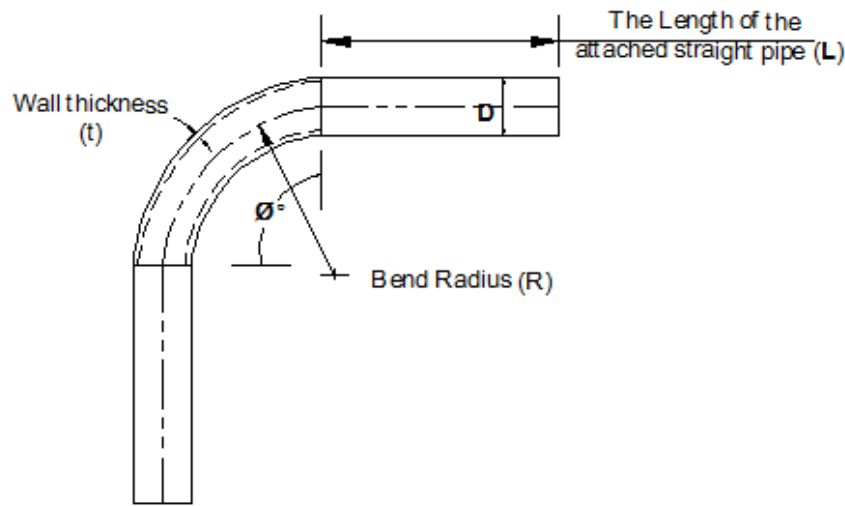


Fig.1. Pipe Bend Geometry

## 2.2 Material properties and Boundary Conditions

The pipe bend along with the straight pipes are acting together as a fixed-free pipe system. A reference point is assigned at one of the straight pipe ends and denoted RP-1 as shown in (Fig.2). This point is fixed while the other end of the pipe system is free to rotate and translate. The circumference of the pipe at the fixed end is tied to RP-1 using a kinematic coupling constraint and the radial translation is allowed to enable the pipe to expand radially under internal pressure. The pipe bend is modeled using a four-node quadrilateral shell element with reduced integration (S4R). A mesh convergence study was conducted and accordingly, the whole pipe system has a mesh size of 15x15 mm. A bending moment is applied at the free end as a rotational displacement of 0.25 radians. The rotational displacement is applied in an increment of 0.05 radians. The pipe system is of steel grade X52 with material properties presented in Table (1).

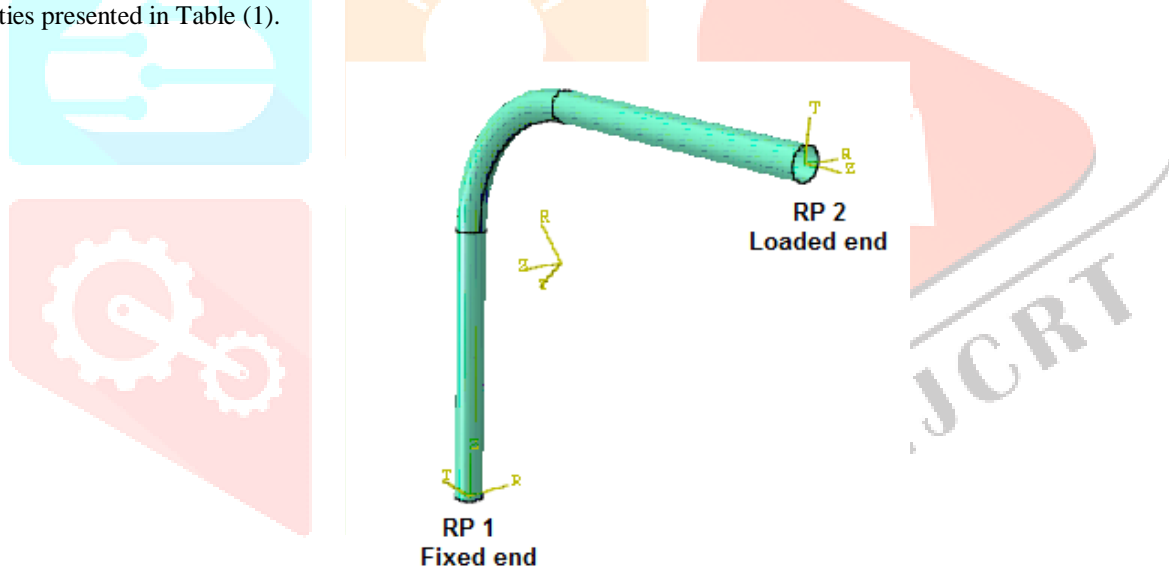


Fig. 2. Model boundary conditions

## 2.3 Loading

The loading is performed in two steps, where the internal pressure is applied on the pipe inner walls in the first step. The bending moment is applied in a second step as a rotational displacement either in an opening or closing direction. The examined results are the hoop, longitudinal, and Tresca stresses which are obtained from the FEA numerical models at the location of critical stresses. These stresses are measured at the outer, inner, and mid-layer through pipe wall thickness.

Table 1: Finite Element Model Parameters

Parameter		Value
D	Pipe diameter	(NPS20)=508mm, (NPS40)=1016mm, (NPS72)=1829mm
L	Pipe length, L=10D	5080mm ,10160mm ,18290mm
t	Wall thickness	9.525, 12.7, 25.4 mm
R	bend radius, mm	1D,3D,5D
R/r	Relative bend radius	2,6,10
D/t	Slenderness ratio	20,40,50,72,80,106,144,200
h	Bend ratio(beam parameter)= $Rt/r^2$	From 0.02 to 1.1
$\emptyset$	Bend Angle, degrees	30°,60°,90°,120°,160°
E	Young's modulus	$2 \times 10^5$ MPa
$\nu$	Poisson's ratio	0.3
Sy	Yield strength of ( steel grade X52 )	360MPa

#### 2.4. Validation of the finite element model

The FEA results are compared to the experimental work of Gross (1953) [1] who conducted an experimental study on short bend radius pipes of thin wall thickness subjected to in-plane external moments. The 90-degree bends are attached to two straight pipes to eliminate any localized end effects due to the method of loading. The tested pipes are vertically and laterally supported at the bottom end, while the top end is free to rotate and translate vertically. The complete test setup can be found in the original published paper by Nicol Gross, 1952 [1], The displacement experimental results from tests "Bend 1" and "Bend 3" are used to verify the FEA model in this current study. The geometry and the pipe size for the tested pipes are presented in Table (2). The testing technique applies a load at both ends that exert a bending moment increasing linearly with distance from the line of loading. The maximum bending moment occurs at the mid-length of the pipe bend being the furthest from the loading line of action. The vertical displacement is measured from these tests and compared to the displacements evaluated from the FEA models for verification.

Table 2: Dimensions of tested pipes (Gross 1953) [1]

Test	NPS	Outer diameter (D,mm)	Wall thickness (t,mm)	Bend radius (R,mm)	Straight pipe length (L,mm)
Bend 1	12	314.706	4.7625	457.2	958.85
Bend 3	6	159.7152	3.175	228.6	611.124

A vertical load is applied at the free end with a value equal to the failure load from the tested pipes. The vertical displacement at the free end is evaluated during loading and compared with the displacement measured from the tests. The results from the FEA are plotted against the results from the tested pipes in Figures (3) and (4). The FEA results show good agreement with the experimental data. Consequently, the FEA model is used in conducting a parametric study on pipe bends considering some minor changes in the verified model such as, adding an end boundary condition or changing the material properties.

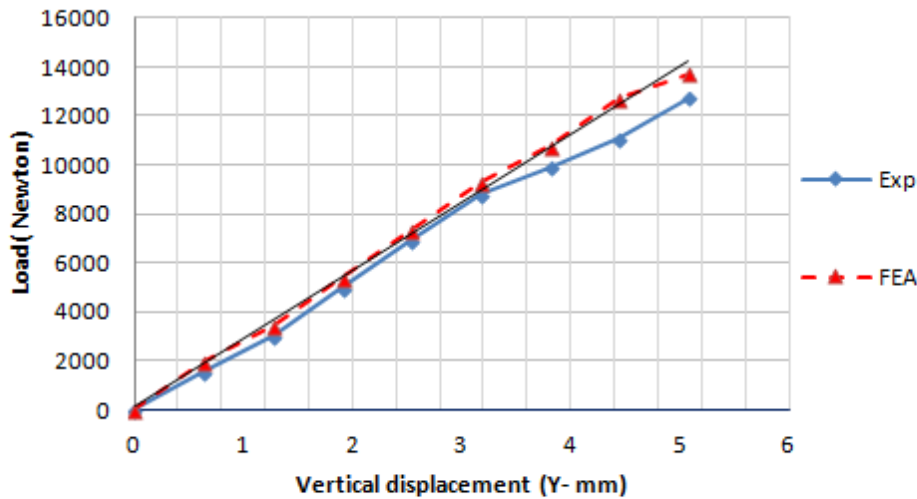


Fig.3. The vertical displacement from FEA vs the experimental results for Bend 1

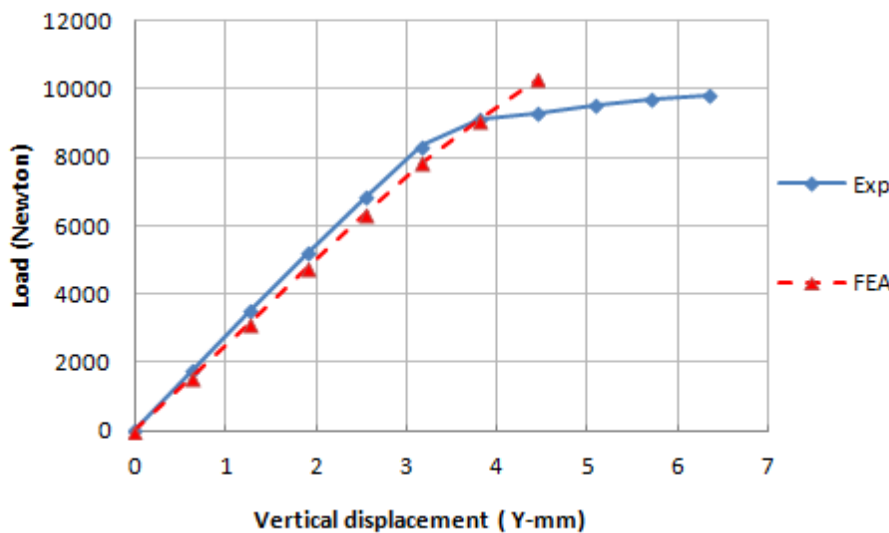


Fig.4. The vertical displacement from FEA vs the experimental results for Bend 3

### III. PARAMETRIC STUDY RESULTS UNDER DIFFERENT LOADINGS

#### 3.1. Under internal pressure

The American design code (ASME B31.1) [5], first provides a method to design a pipeline system under pressure and other external loadings or the nominal wall thickness for a given design pressure shall be determined by the following Equation (1), and after that, the combined stresses are checked against the code limitations according to the given loading conditions.

$$P = \frac{2St}{D} \text{ FET} \tag{1}$$

Where:-

S = SMYS (Specified minimum yield strength)

F = design factor from the table in ASME

E = longitudinal joint factor obtained from the table in ASME

T = temperature derating factor obtained from the table in ASME

P = design pressure, MPa

D = nominal outside diameter of the pipe, mm

t = nominal wall thickness, mm

The combined stresses according to the code are shown to be the difference between the hoop stress and the net longitudinal compressive stress which is twice the maximum shear stress. For pipe bends subjected to internal pressure only, the longitudinal stress is ignored since it results in tensile stress. Therefore, the combined stress is equal to the hoop stresses.

The Tresca stresses are extracted from the FEA model as they are defined as the difference between the hoop and longitudinal stress in this case at the location of maximum stresses and compared to the estimated combined stress using the ASME B31.1 Equation (2) as follows:

$$(S_h - S_L) \leq 0.9 S * T \tag{2}$$

Where:-

S<sub>h</sub> = Hoop stress due to design pressure, MPa.

S<sub>L</sub> = Longitudinal compression stress, MPa.

S = yield stress value at design maximum temperature from code Tables, MPa.

Equation (2) represents the value of combined stresses which is presented in the ASME-B31.1 equal to the highest absolute value of the difference between hoop stress (S<sub>h</sub>) and the longitudinal stress (S<sub>L</sub>) is considered to be less than or equal to 90% of yield strength at maximum temperature, which shows an absence of differentiation between straight pipes and pipe bends in the ASME code. Therefore, Finite Element Modeling (FEM) is used to judge the increase in stresses on pipe bends subjected to internal pressure compared to straight pipes.

### 3.1.1 The shape of cross-sectional deformation under internal pressure loading only

Fig.5.shows the distribution of Tresca stresses along half of the pipe cross-section starting from the intrados (Θ=0°) going to the extrados (Θ = 180°). These stresses are evaluated at the mid-section of the pipe.

The stresses are found to be higher at the outer surface of the pipe at the intrados and extrados locations. However, the inner surface of the pipe has higher stresses at the crown location and this depends on the shape of ovalization.

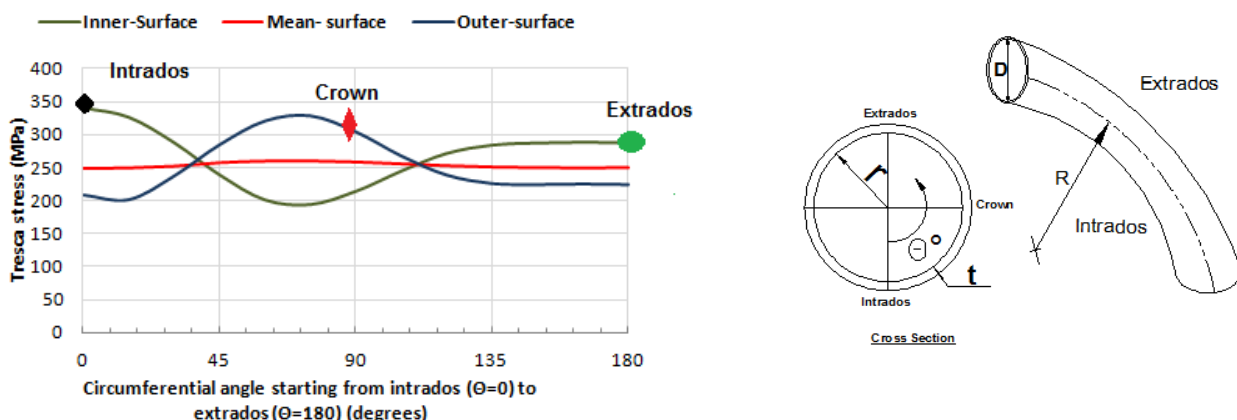


Fig.5.The distribution of Tresca stresses along the circumference of half the pipe cross-section at the mid-section of pipe bend for Shell element model.

### 3.1.2 Evaluation of the stress distribution and the maximum stress location along the pipe bend circumference compared to ASME B31.1

The Tresca stresses are twice the maximum shear stress and since the longitudinal stress is in tension, the maximum shear stress is based on the hoop stresses only. Therefore, the Tresca stresses are always equal to the hoop stresses under internal pressure loading only. The hoop stress distribution is a result of the bending of the pipe wall. Therefore, the shape of the cross-sectional deformation can be identified from the hoop stress distribution.

In the case of bend angle ( $\phi$ ) = 30° with a small bend diameter of NPS 20 (508mm), it can be concluded that the hoop stress at the inner surface has significant stress increase greater than the ASME – code stresses with a percentage of 49.3% at the intrados location and while the outer surface is greater than the code stresses with a percentage of 42.3% at the crown location. The hoop stress has the least stresses at the mean surface which is greater than the ASME – code stresses with a percentage of 4.86% at the crown location which is nearer to the behavior of the straight pipe as per Fig.(6)

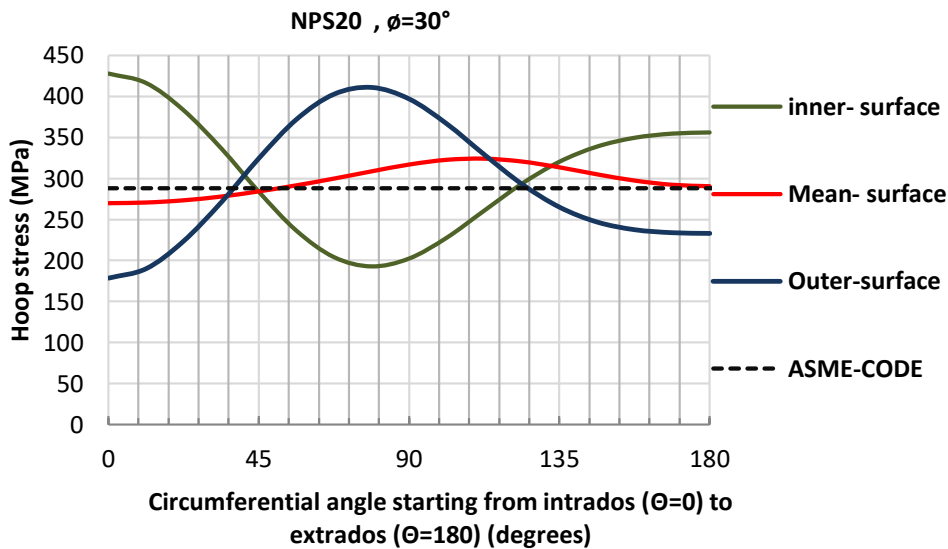


Fig.6. Hoop stress distribution along the circumference of the critical section of an NPS20 pipe bend with a small angle of 30°

However, for pipe bends with the same bend angle ( $\phi$ )=30°, but with a large bend diameter of NPS 72 (1829mm), it can be concluded that the hoop stress at the inner surface is greater than the ASME – stresses with a percentage of 18.1% at the intrados location. And at the outer surface, with almost the same percentage of 18.066% but at the crown location, while the hoop stress at the mean surface shows the least percentage of 13.2% at the crown location of the pipe bend as shown in Fig.(7).

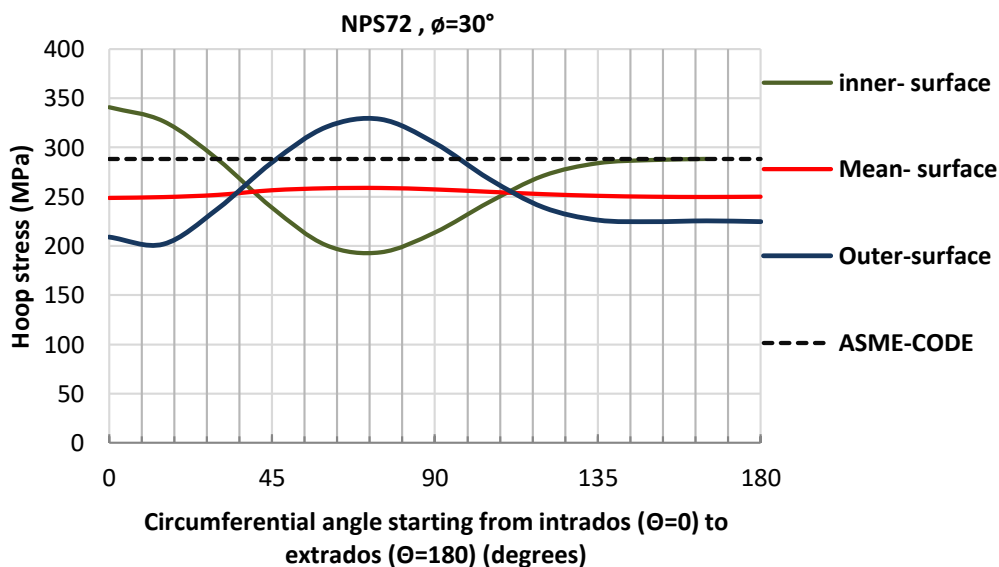
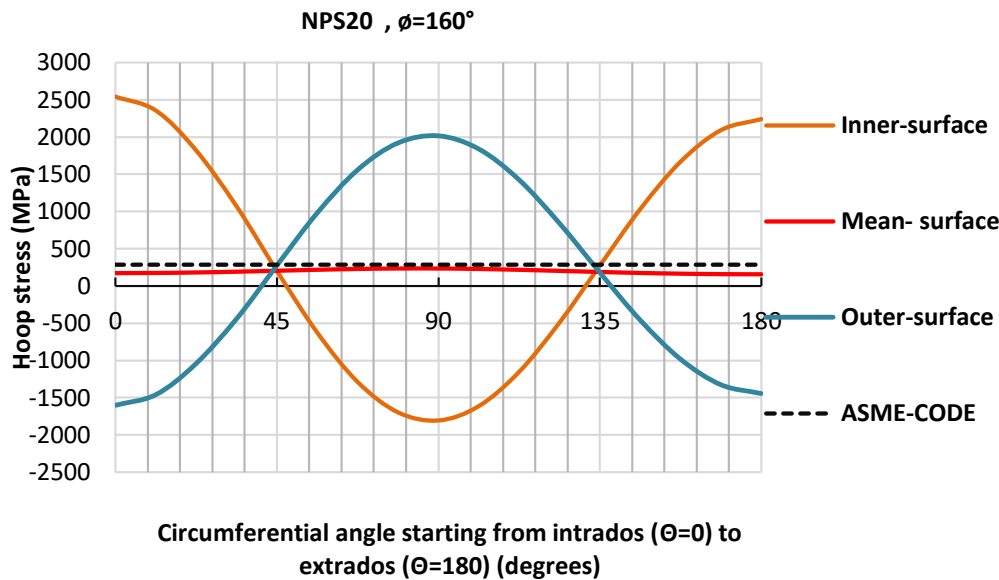


Fig.7. Hoop stress distribution along the circumference of the critical section of an NPS72 pipe bend with a small angle of 30°

In Fig.(8) at bend angle ( $\phi$ )=160° with a small bend diameter of NPS 20 (508mm), it can be concluded that, at both the inner and outer layers of the pipe bend wall, the hoop stresses show a significant increase at the intrados zone where the circumferential angle is zero degrees than the ASME – code stresses, while The hoop stress at the mean surface is almost equal to the ASME – code stresses with a percentage of 1.1% at the crown location which is nearer to the behavior of the straight pipe.



**Fig.8.** Hoop stress distribution along the circumference of the critical section of an NPS20 pipe bend with a large angle of 160°

While at the same bend angle (φ)=160° with a large bend diameter of NPS 72 (1829mm), it can be concluded that the hoop stresses at the outer and inner surfaces where the circumferential angle is around 45 to 90 degrees at the crown zone are greater than the ASME – code stresses with a percentage of 250.69 %. however, the hoop stress at the mean surface hoop shows the least percentage of 13.2% than the ASME – code stresses at the crown location as shown in Fig.(9).

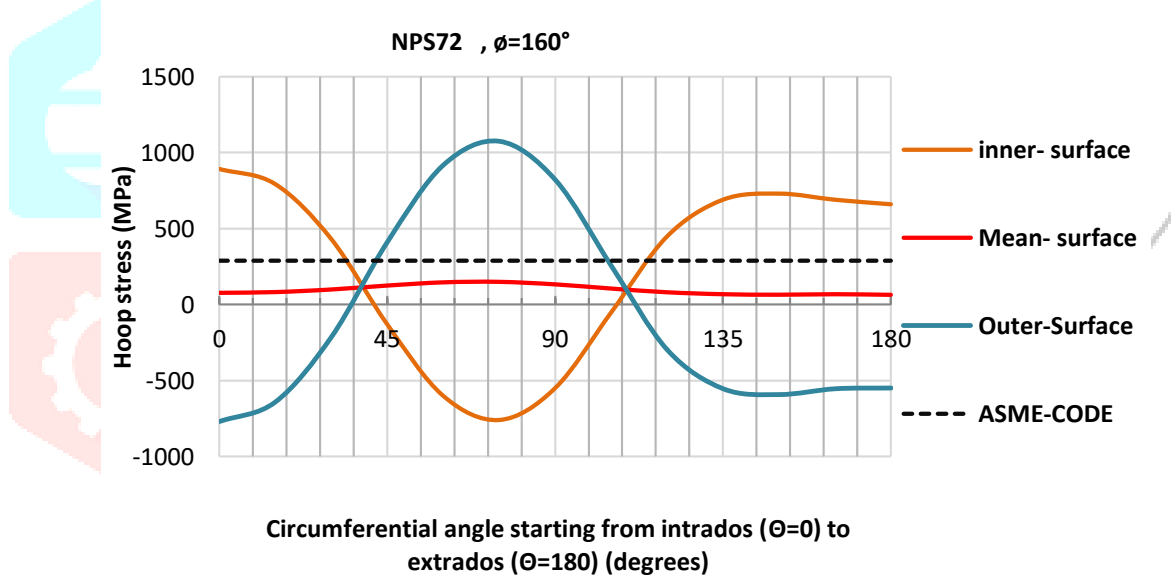


**Fig.9.** Hoop stress distribution along the circumference of the critical section of an NPS72 pipe bend with a large angle of 160°

from the studied cases above, it can be concluded from the hoop stress results shown in Figures from (6) to (9) that the intrados and extrados are pulled further away from the pipe center while the crown is pushed towards the center of the pipe cross-section resulting in an oval shape with the major axis is in the plane of symmetry and as the bend angle increases with the same bend size the stress variation between outer and inner layers increase, depending mostly on which layer we are studying. Moreover, the outer and inner surfaces carry a maximum stress percentage than the mean surface.

Different bend radii (R) were studied to illustrate their effect on maximum stresses in combination with bend ratios (h) ( from (0.02 to 1.1) and a wide range of bend angles (φ), Pipe bend flexibility is expressed clearly by the pipe bend ratio  $h = \frac{Rt}{r^2}$ .

In Fig.(10) For the short bend radius pipes (R= 1D) the critical case is the pipe bends with bend angles 160 and 120 degrees where the maximum Tresca stress is 430.33, 425.1 MPa; respectively. The estimated combined stresses using ASME standards is 288 MPa for all bends. Since the code equation ignores the bend angle and bend radius. However, the FEA results show that the internal pressure effect has a significant effect of an increase in the combined stress by up to 49.3% for short bend radius pipes.



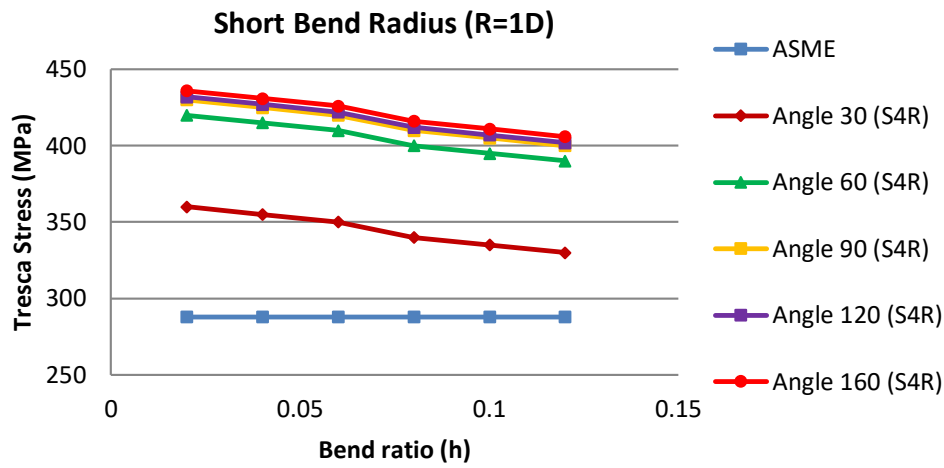


Fig.10. Tresca stress result from the Shell model vs ASME for short radius bends Subjected to internal pressure causing 80% SMYS hoop stress.

While, in Fig.(11) For the long bend radius pipes (R= 5D), the highest Tresca stress was found to be with a bend angle of 160 degrees. The maximum stress is 305.6 MPa while the combined stress estimated using ASME is 288 MPa. However, the FEA results show that the internal pressure effect shows the least stress increase in the combined stress by up to 6.11% for long bend radius pipes.

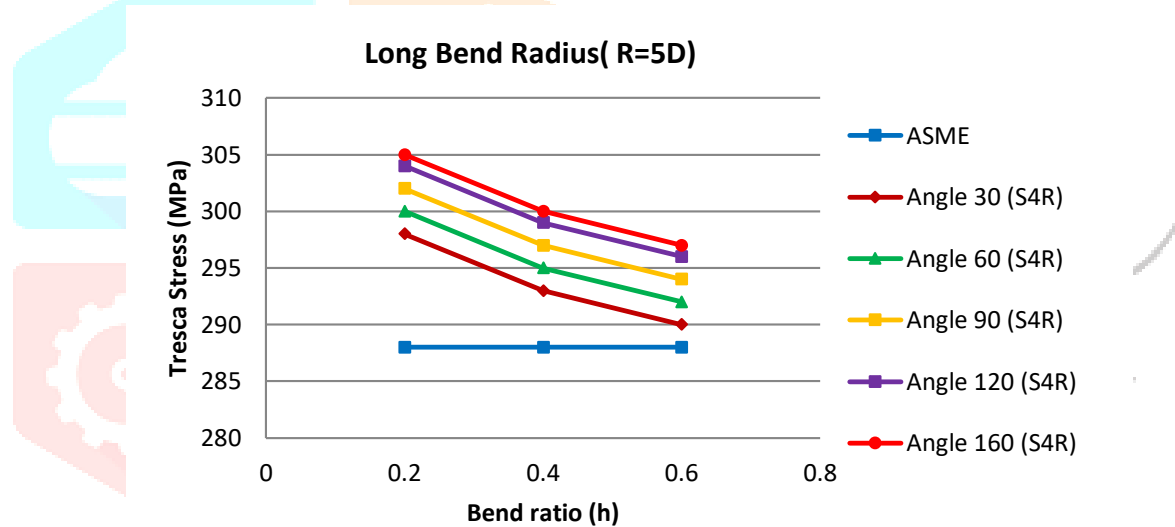


Fig. 11. Tresca stress result from the Shell model vs ASME for long radius bends Subjected to internal pressure causing 80% SMYS hoop stress.

Therefore, we can conclude that, as the bend radius increases, the pipe bend tends to act like a straight pipe and the FEA stresses are closer to the ASME code estimated stresses using Barlow’s equation ( $\sigma=PD/2t$ ) which was derived for straight pipe. Therefore, as the bend tends to act as a straight pipe due to the large bend radius, the stresses will get closer to the ASME estimated stresses. The FEA results show that the combined stresses evaluated using the ASME equation are un-conservative since the actual stress on the pipe bend reaches up to 1.5 times the estimated stress for a short radius (R=1D).

Fig.(12) shows the results for each pipe bend with different bend angles varying from 30° to 160°. Since the ASME – code does not consider the bend angle in estimating the combined stress, therefore, the combined stress is found to be constant for different bend angles. The FEA results show that the maximum increase in Tresca stresses is 13.7 % with bend angles from 30 to 90 degrees. However, the Tresca stress shows the least increase by 4.18 % when the bend angle increase from 90 to 160 degrees. Therefore, we can conclude that as the bend angle increase, the stresses increase by a maximum of 15.58% for short bend radius pipes, and for long bend, radius pipes are found to be almost with no change by 1.86% for long bend radius pipes.

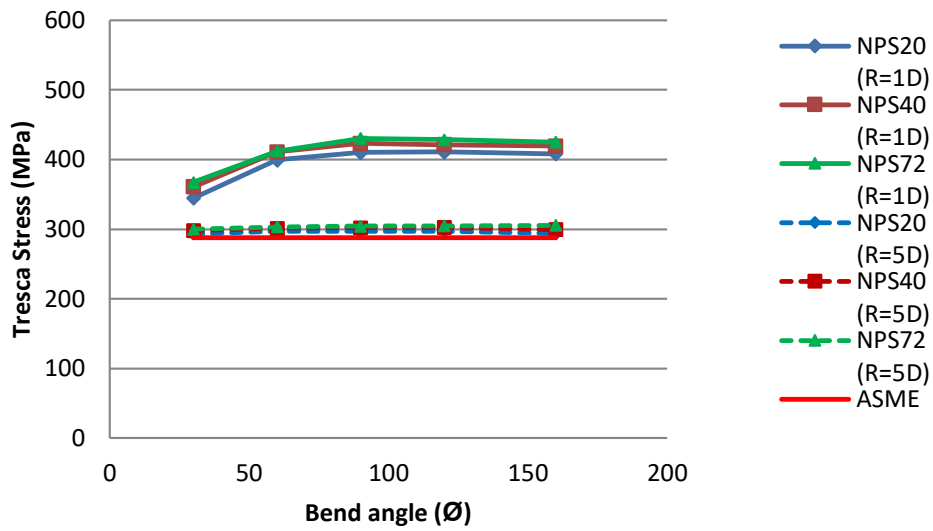


Fig.12. Tresca Stress result vs the bend angle for different pipe bend sizes subjected to internal pressure causing 80% SMYS hoop stress.

### 3.2. Under Pure in-plane bending moment (closing and opening)

A pipe bend subjected to bending moment will show membrane deformations in the cross-section. The shape of cross-sectional deformation (ovalization) depends on the direction of the bending moment. The cross-section either flattens or ovalizes.

the ASME B31.3 code [6] estimates the stresses based on the bending moment at the mid-layer along with the pipe bend thickness, but it neglects the effect of both bending moment direction, and bend angle ( $\theta$ ) on the stresses, so the Von Mises stress results are conducted at the mid-layer vs the reaction moment for a pipe bend with an NPS20, and NPS72 outer diameter with short pipe bend radius ( $R = 1D$ ) to study the effect of bending moment direction and bend angle on stresses. as shown in Figures (13) and(14).

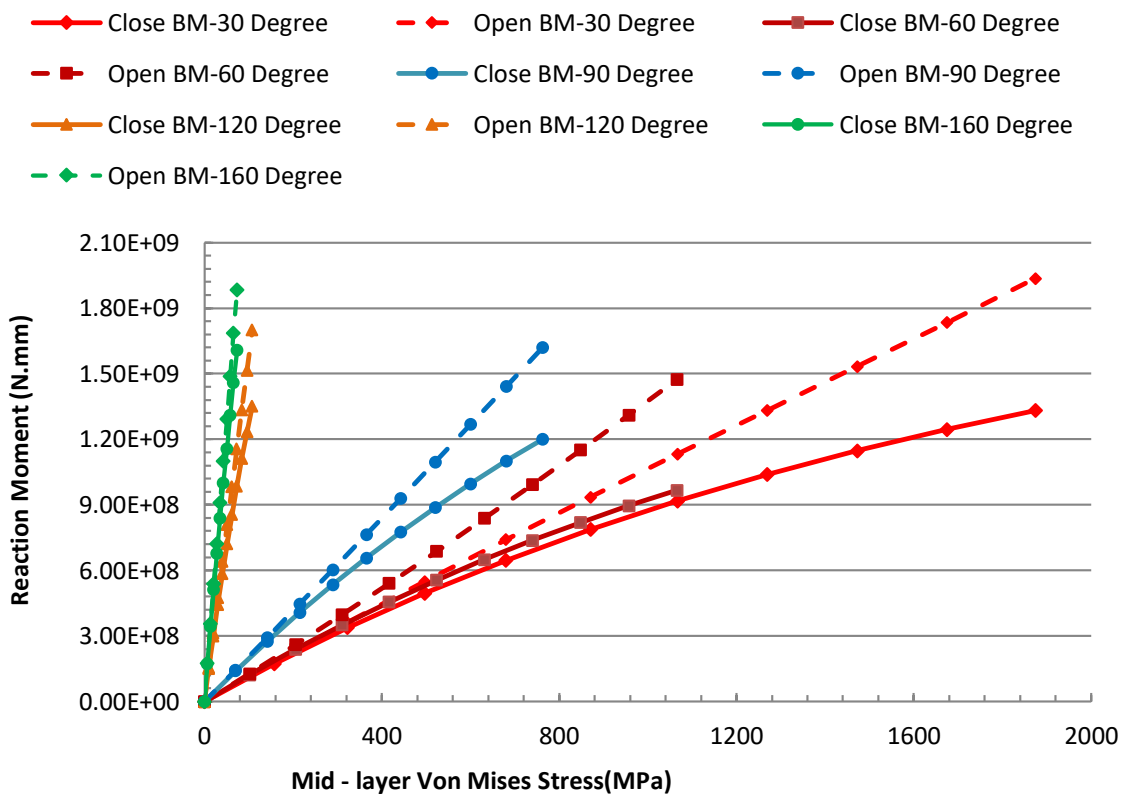


Fig.13. Von Mises stress vs reaction moment for NPS 20 pipe with short bend radius R=1D

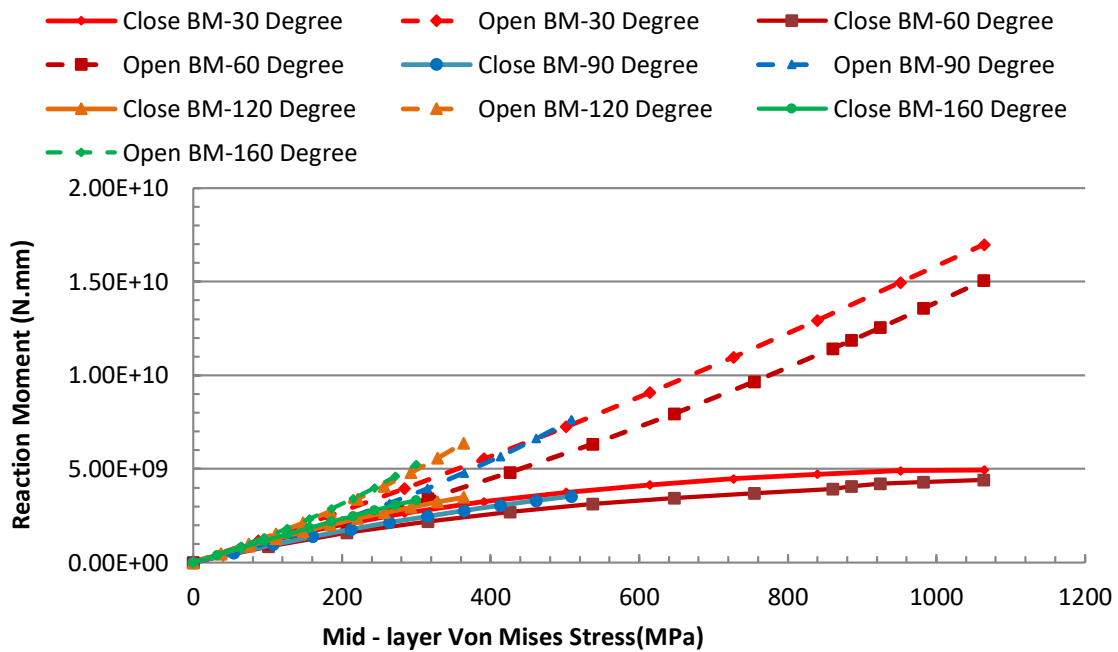


Fig. 14. Von Mises stress vs reaction moment for NPS 72 pipe with short bend radius R=1D

We can conclude that at the same bending moment, the Von Mises stress on a pipe bend with a small bend angle is lower than that of a large bend angle pipe. In addition to that, changing the bend angle from 30 to 160 degrees causes an increase in the von Mises stress by 80% at the mid-layer of the pipe wall thickness. Consequently, this shows that the bend angle has a significant effect on the Von Mises maximum stress measured on the pipe bend. Besides, changing the direction of bending moment affects the Von Mises stress since it affects the pipe flexibility. By applying a closing bending moment results in higher stresses than that of an opening bending moment by up to 45% in this studied case.

3.2. 1 The Effect of the direction of the applied bending moment on pipe bend stress distribution

The Von Mises stress is equivalent stress that is a function of the differences in the principal stresses, which are considered the longitudinal and hoop stress in this study. Therefore, the maximum Von Mises stress location depends on the maximum longitudinal and hoop stress locations. Figures from (15) to (20) for short bend radius, and from (21) to (28) for long bend radius show the distribution of the Von Mises stress, hoop stresses, and longitudinal stresses across the circumference of the pipe bend from intrados ( $\theta = 0$ ) to extrados ( $\theta = 180$ ) on the inner, outer, and mid-layer.

Figures (15),(16) show the stress distribution on a 90-degree pipe bend with NPS 20 outer diameter ( $D=508$  mm with  $t=9.525$ mm) and short bend radius ( $R = 1D$ ) subjected to an opening and closing bending moment. This case is considered one of the typical stress distribution cases for pipe bends.

The FEA results showed that the distribution of the Von Mises stress on the mid-layer of the pipe bend has two maximum points. The two peaks are approximately at a circumferential angle ( $\theta$ ) of 45 and 135 degrees. while, for the inner and outer layers, the maximum Von Mises stress is found to be always at the crown location ( $\theta = 90$  degrees) regardless of the direction of applied end rotational displacement.

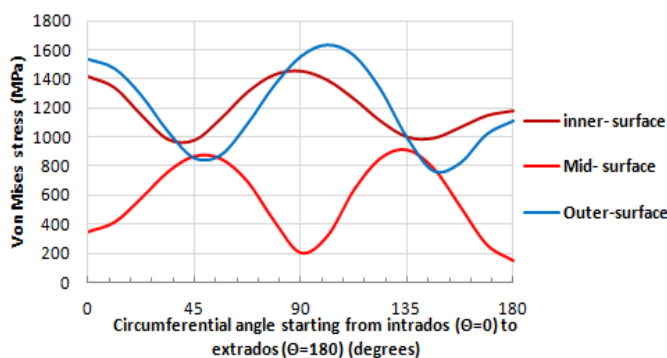


Fig. 15. Von Mises stress distribution along the critical section of a pipe bend NPS 20 with bend angle 90° and short bend radius ( $R = 1D$ ) subjected to an opening bending moment

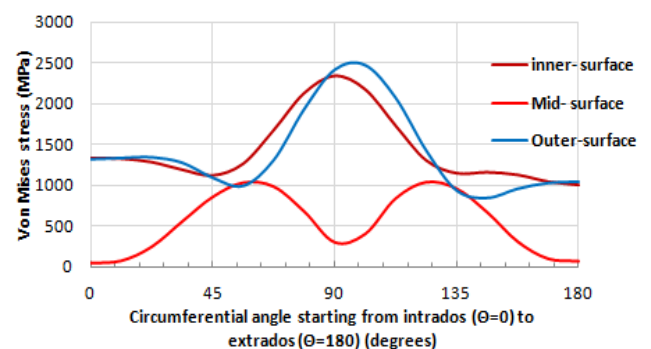
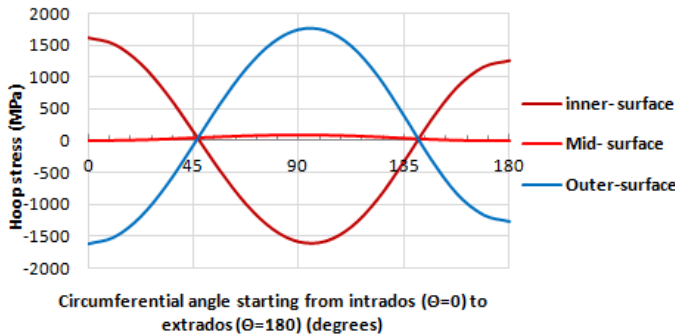


Fig.16. Von Mises stress distribution along the critical section of a pipe bend NPS 20 with bend angle 90 ° and short bend radius ( $R = 1D$ ) subjected to a closing bending moment

On the other hand, the hoop and longitudinal stress distributions are affected by the bending moment direction. The ovalization of the cross-section adds bending stresses on the pipe wall that mainly affects the hoop stresses. For the case of an opening bending moment, Figures (17) and (18) show the hoop stress distribution on the critical section where the maximum stress is found to be at the crown location for all three layers; inner, outer, and mid-layer of the wall thickness.

Figures (17), at the inner layer of the pipe wall, the hoop stresses are compressed at the crown zone where the circumferential angle is around 45 to 135 degrees, while the rest of the outer layer is in tension. However, the opposite is for the outer layer, where the hoop stresses are tension at the crown zone and compression at the intrados and extrados of the bend as shown in Figure (18).

The hoop stresses at the mid-layer of the pipe wall are considered negligible when compared to the stresses found at the inner and outer layers regardless of the direction of the bending moment. The maximum hoop stress is found to be at the inner layer of the pipe wall in all typical models.



**Fig .17.** Hoop stress distribution along the critical section of a pipe bend NPS 20 with bend angle 90°and short bend radius (R = 1D) subjected to opening bending moment.

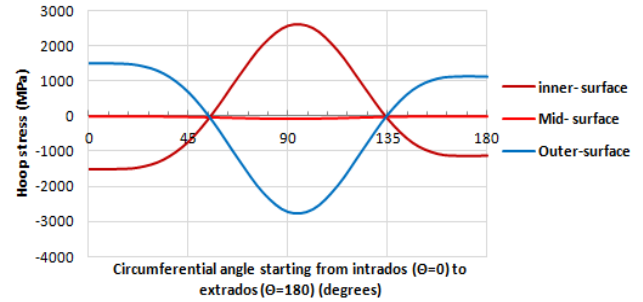


**Fig .18.** Hoop stress distribution along the critical section of a pipe bend NPS 20 with bend angle 90°and short bend radius (R = 1D) subjected to closing bending moment.

Figures (19) and (20), show the maximum longitudinal stress distribution for a pipe bend subjected to an opening bending moment at the critical section is found to be in two different regions in the pipe bend.

The first region is between the intrados and the crown of the pipe bend approximately between a circumferential angle of 33 and 67 degrees, while the second region is between the extrados and the crown between approximately 123 and 146 degrees as shown in Figure (19). The longitudinal stresses across the wall thickness are found to be tension at the intrados area and compression at the extrados area. However, when a closing bending moment is applied, the stresses are mirrored in the opposite direction to be tension at the extrados and compression at the intrados as shown in Figure (20).

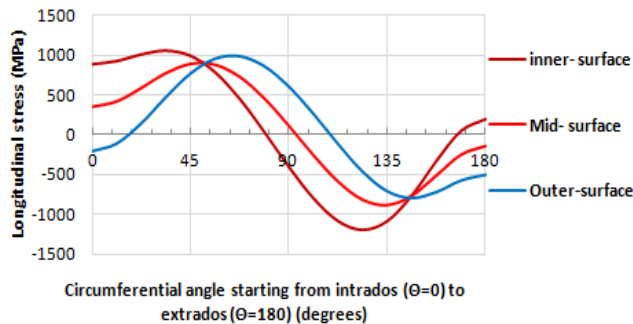


**Fig.19.** Longitudinal stress distribution along the critical section of a pipe bend NPS 20 with bend angle 90 °and short bend radius (R = 1D) subjected to opening bending moment.

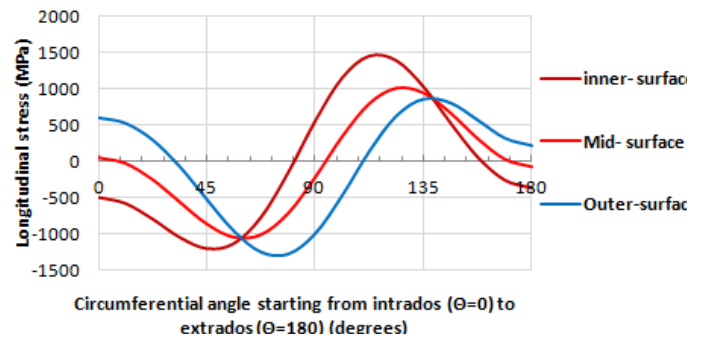


**Fig.20.** Longitudinal stress distribution along the critical section of a pipe bend NPS 20 with bend angle 90 °and short bend radius (R = 1D) subjected to closing bending moment.

The results from all the studied above models show that the maximum Von Mises stress through the wall thickness is at the inner layer of the pipe wall at the crown location. as shown in Figures (15) & (16). Therefore, it is expected that for higher stresses, the inner surface of the pipe bend will start yielding.

We can conclude that the design of pipe bends should not be restricted to the stresses at the mid-layer of the wall thickness only, these results and conclusions show good agreement with Gross's (1953) experimental results, which investigated that the circumferential stresses( hoop stresses) are the main reason behind pipe bend failure.

Figures from (21) and (26), in the case of pipe bend with a long bend radius (R= 5D). The maximum hoop and longitudinal stress are at the intrados for all three layers for small pipe size (NPS 20), (NPS 40), (NPS 72), and a small bend angle of 10 degrees (this small acute angle is used for research purposes only)with a long bend radius (R= 5D) are studied representing the effect of small bend angle.

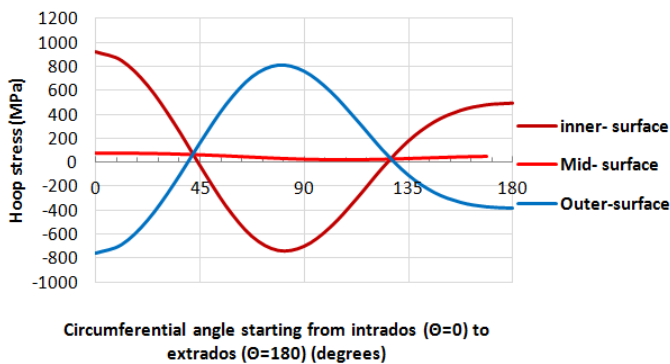


**Fig .21.** Hoop stress distribution along the critical section of a pipe bend NPS 20 with bend angle 10° and long bend radius (R = 5D) subjected to opening bending moment.

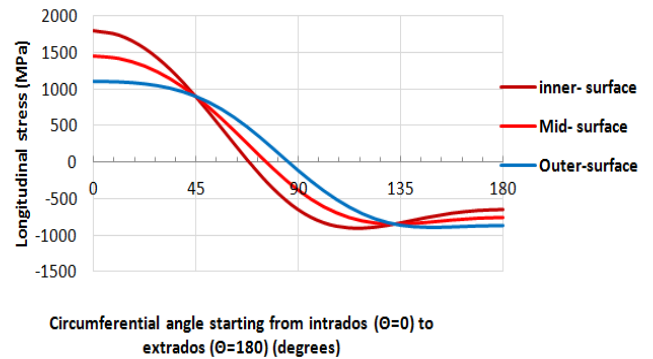


**Fig.22.** Longitudinal stress distribution along the critical section of a pipe bend NPS 20 with bend angle 10 ° and long bend radius (R = 5D) subjected to opening bending moment.

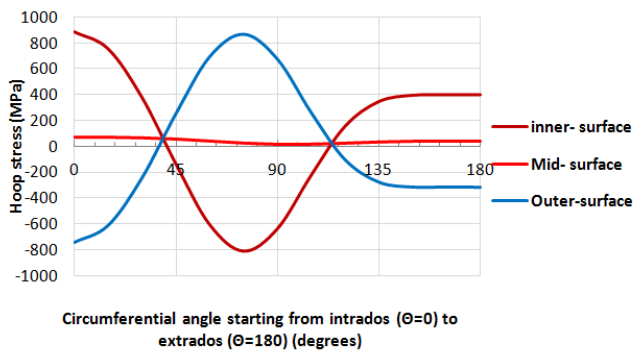


**Fig.23.** Hoop stress distribution along the critical section of a pipe bend NPS 40 with bend angle 10° and long bend radius (R = 5D) subjected to opening bending moment.

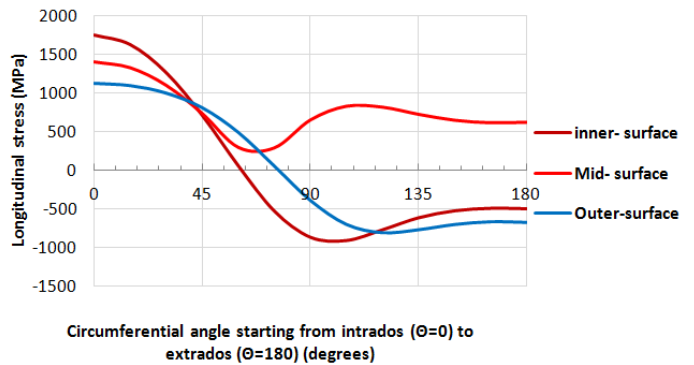


**Fig.24.** Longitudinal stress distribution along the critical section of a pipe bend NPS 40 with bend angle 10 ° and long bend radius (R = 5D) subjected to opening bending moment.

For long radius pipe bends (R = 5D), with large pipe size (NPS 72), the behavior act as a straight pipe since the maximum longitudinal stresses are at the max point away from the center of the pipe which is the intrados and extrados. As the pipe size increase to NPS 72, the location of maximum hoop stress for the inner and outer layers are located at the crown as shown in Figure (25). While the maximum hoop stress at the mid-layer is around a circumferential angle of 45 degrees and is considered negligible compared to the stresses found at the inner and outer layers.

In Figure(26) The longitudinal stress for the inner layer is around 65 degrees while the outer layer is at the crown. The mid-layer has two maximum longitudinal stress locations around 45 and 120 degrees and is found to be as high as the inner and outer layers. therefore, The hoop stresses at the inner and outer layers govern the Von Mises stress in the case of large pipe sizes such as NPS 72.

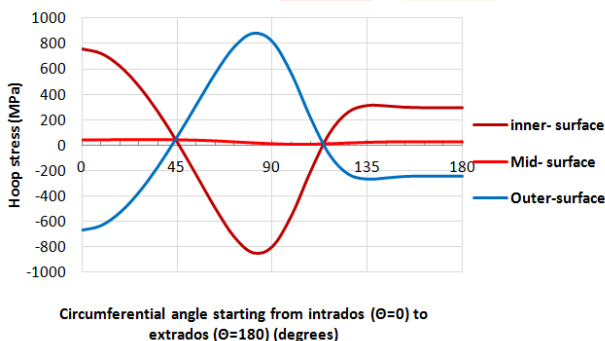


**Fig .25.** Hoop stress distribution along the critical section of a pipe bend NPS 72 with bend angle 10° and long bend radius (R = 5D) subjected to opening bending moment

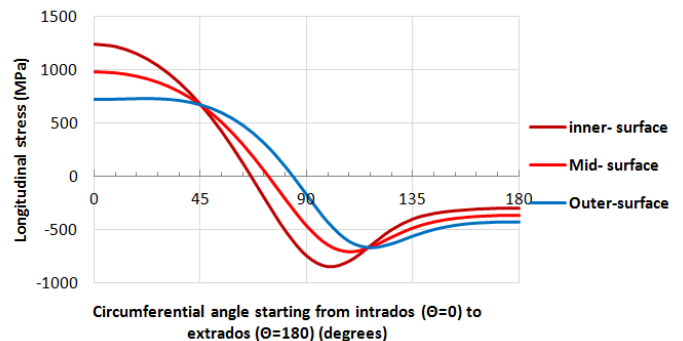


**Fig. 26.** Longitudinal stress distribution along the critical section of a pipe bend NPS 72 with bend angle 10 ° and long bend radius (R = 5D) subjected to opening bending moment

Figures (27), (28) show that the inner and outer layers have maximum Von Mises stress similar to the hoop stress at the crown location while the mid-layer is governed by the longitudinal stress therefore there are two local maximum stresses locations. Therefore we can conclude that The Von-Mises stress depends on the highest of stresses between both, the hoop and longitudinal stress. Therefore, the hoop and longitudinal stresses must be considered in the design of pipelines.

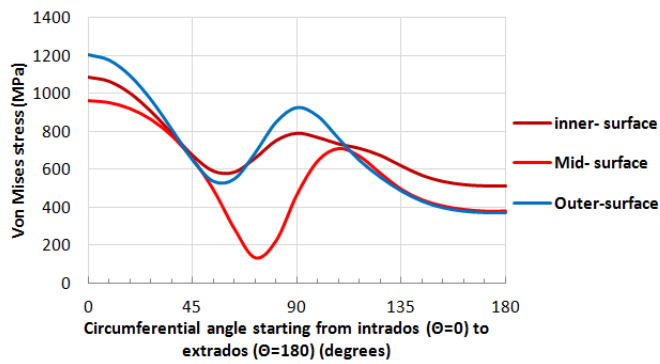


**Fig.27.** Von Mises stress distribution along the critical section of a pipe bend NPS 72 with bend angle 10 °and long bend radius (R = 5D) subjected to an opening bending moment

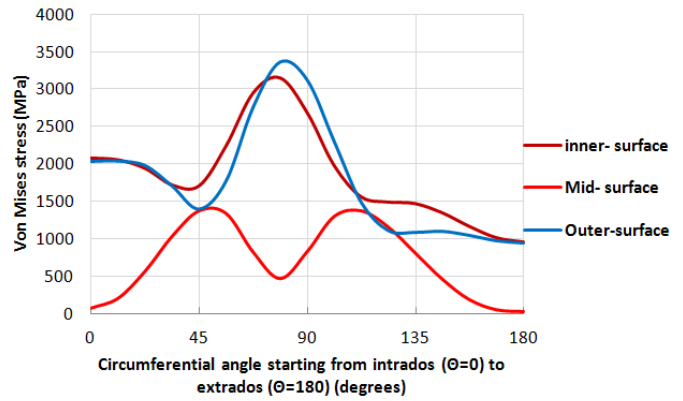


**Fig.28.** Von Mises stress distribution along the critical section of a pipe bend NPS 72 with bend angle 10 °and long bend radius (R = 5D) subjected to an opening bending moment

**3.2.2 The Effect of the direction of bending moment on pipe bend (flexibility and stiffness)**

To investigate the behavior of the pipe bend, the relationship between the applied end rotation versus the generated reaction moment is studied.

For short radius (R=1D), pipe bends with NPS 20 and NPS 72 outer diameter, and with a range of bend angles from 30 to 160 degrees were investigated. The relation between the end rotation and reaction bending moment is found to be linear in the case of pipe bends with small pipe sizes as NPS 20 Fig. (29). However, as the pipe bend size increases to NPS 72, the relationship tends to be slightly non-linear as shown in Fig.(30). It is found that by applying an opening end rotation, the results have a concave upward curve where the rate of increase in the reaction moment increases throughout the loading and consequently, this means that the pipe bend gains stiffness and loses flexibility with loading. However, the case of applying a closing end rotation shows that the results have a concave downward curve, which shows that the pipe bend starts to lose its stiffness and flexibility increases.

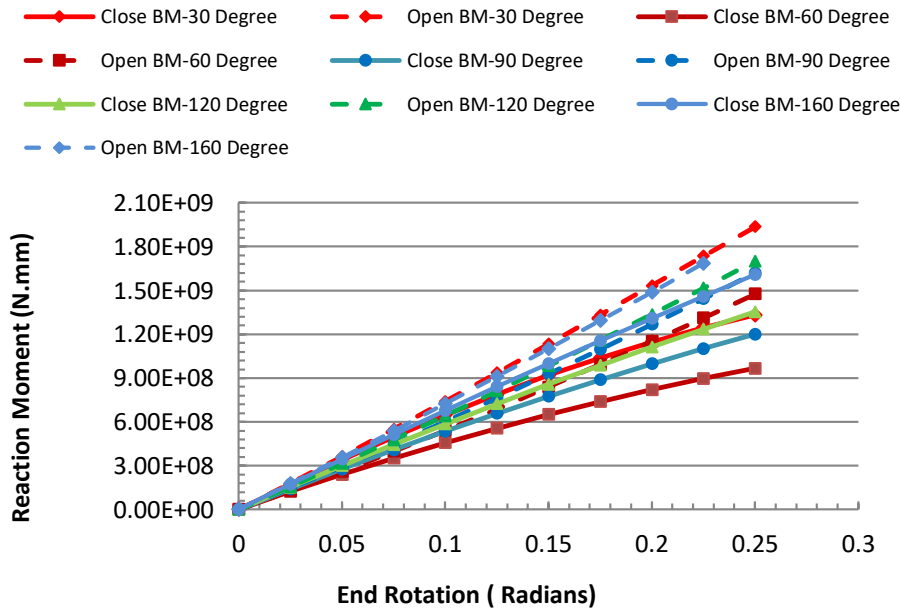


**Fig.29.** End rotation vs reaction moment for NPS 20 with short bend radius (R=1D).

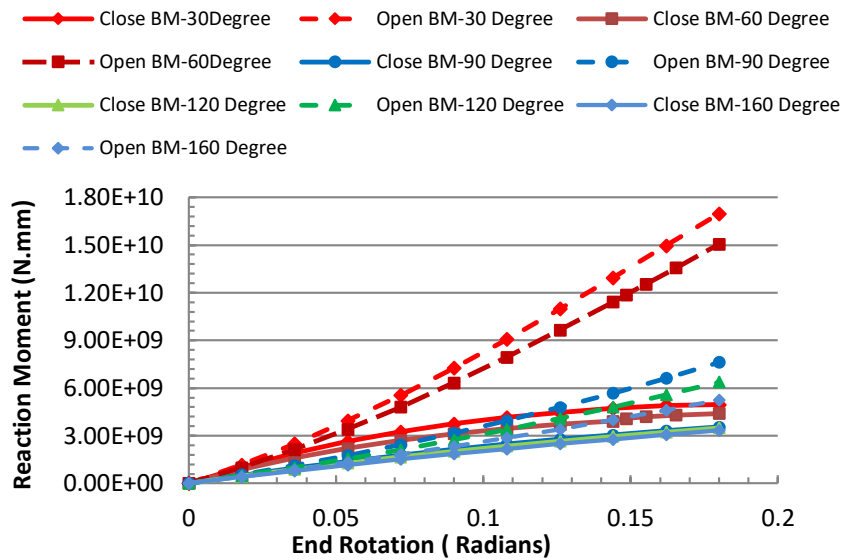


Fig.30. End rotation vs reaction moment for NPS 72 with short bend radius (R=1D).

For long radius (R=5D), the relationship between the end rotation and reaction moment is linear as shown in Figures (31) and (32). Figures from (29) to (32) show that at the same bending moment, the small bend angle pipes have a smaller end rotation than large bend angle pipes. This means that as the pipe bend angle increases, the pipe bend becomes more flexible therefore tends to have higher deformations under the same applied load.

Moreover, at the same bending moment, the end rotation resulting from the opening bending moment is lower than the end rotation resulting from the closing bending moment. In addition to that, the bending moment required to rotate the pipe bend with a particular end rotation (0.25 radians) in the opening direction is up to 2.5 times higher than that required for the closing direction.

Therefore, pipe bends subjected to closing bending moments are more flexible than those subjected to opening bending moments, and the flexibility of a pipe bend changes by changing the direction of the applied bending moment.

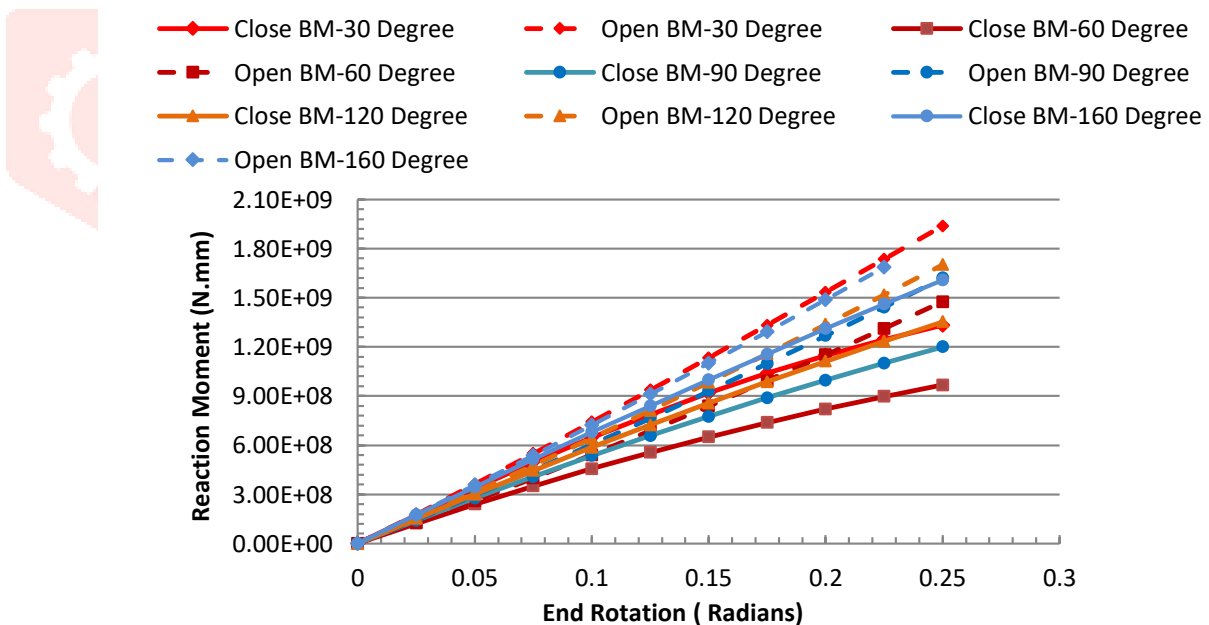


Fig. 31. End rotation vs reaction moment for NPS 20 with long bend radius (R=5D).

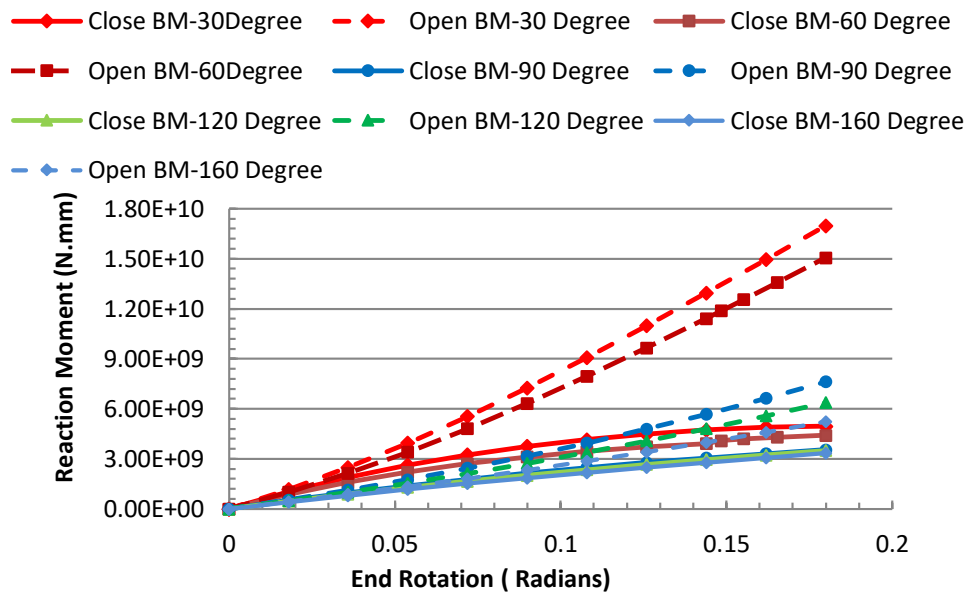


Fig.32. End rotation vs reaction moment for NPS 72 with long bend radius (R=5D).

#### IV. SUMMARY AND CONCLUSIONS

By comparing the behavior of the studied pipe bends geometries to each parameter, Pipe bend angle ( $\theta$ ) and the direction of bending moment have a great effect on the behavior of pipe bends (flexibility, stiffness, and stresses) for both short radius pipes (1D) and long radius pipes (5D).

**This current study investigated the large diameter pipe bends in comparison to the past studies of small pipe bends. The following are the conclusions from the current study;**

- As the bend radius increases, the pipe bend approaches the behavior of a straight pipe, This is often associated with the bend ratio (h) as well, since the bend ratio increases when the bend radius increases, leading to lower flexibility, thus the observed stresses decrease.
- Pipe bends with small bend angles (10 and 30 degrees) will start yielding at the outer layer of the wall thickness. While, pipe bends with large bend angles (60, 90, 120 & 160 degrees) will start yielding at the inner layer of the wall thickness. Therefore, the design of pipe elbows should be based on the stresses at the inner and outer layers rather than the mid-layer of the pipe wall thickness. This approach aims to provide a design criterion that maintains the pipeline safety and integrity as well as the safety of the environment.
- The direction of bending moment affects the shape of cross-sectional deformation of pipe bends. It flattens when pipe bends are subjected to a closing bending moment. However, the cross-section deforms to an oval shape if subjected to an opening bending moment which eventually affects the hoop stress distribution across the pipe cross-section. The design needs to consider the critical locations of intrados and extrados based on the bending moment direction. As the results showed, the opening moment has max stress at (intrados) while the closing has maximum stress at the (extrados).
- The stiffness of the pipe bend is found to be affected by the deformation shape of the cross-section and this was observed using the reaction moment versus the end rotation curves for both short and long radius pipe bends, When a pipe bend is subjected to an opening bending moment, the stiffness increases as the load increase. However, the stiffness decreases in the case of applying a closing bending moment. Therefore, the flexibility factors presented in the current codes and standards need to be modified to consider the bending moment direction.



## V. REFERENCES

- [1] Gross, N., 1952–1953, “Experiments on Short-Radius Pipe Bends,” Proc. Inst. Mech. Eng., 1.B., pp. 465–479.
- [2] Von Karman, Th. - 1911: Ueber die Formänderung dünnwandiger Rohre, insbesondere fedemder Ausgleichrohre. Zeitschrift des Vereines deutscher Ingenieure, Vol. 55, Part 2, pp. 1889 - 95.
- [3] E.CRodabaugh, H.George, Louisville,1957: Effect of internal pressure on flexibility and stress-intensification factors of curved pipe or welding elbows, MechanicalEngineering News for the power,
- [4] ABAQUS Version 16.6 User’s manual. Inc. and Dassault Systemes; 2016.
- [5] ASME B31.1: Power piping. ASME Code for pressure piping.
- [6] ASME B31.3: Process piping code. ASME Code for pressure piping. petrochemical, and related industries. McGraw Hill.
- [7] Abdulhameed, D., Adeeb, S., Roger, C., Martens, M. 2016. The influence of the Bourdon effect on pipe elbow. Proceedings of the 2016 11th International Pipeline Conference, Calgary, Alberta, Canada.

